Synthesis and characterization of poly(propylene terephthalate/2,6-naphthalate) random copolyesters

C. Lorenzetti[a], L. Finelli[b], N. Lotti[b,*], M. Vannini[b], M. Gazzano[c], C. Berti[b], A. Munari[b]

[a]*Dipartimento di Discipline Economico Aziendali, Area Tecnologia e Valorizzazione delle Risorse, Università di Bologna, Piazza Scaravilli 2, 40126 Bologna, Italy*
[b]*Dipartimento di Chimica Applicata e Scienza dei Materiali, Università di Bologna, Viale Risorgimento 2, 40136 Bologna, Italy*
[c]*Istituto per la Sintesi Organica e la Fotoreattività, CNR, Via Selmi 2, 40126 Bologna, Italy*

Abstract

Poly(propylene terephthalate/2,6-naphthalate) random copolyesters (PPT-PPN) were synthesized and characterized from the molecular and thermal point of view. All the polymers showed a good thermal stability. The main effect of copolymerization was a lowering in the crystallinity and a decrease of T_m respect to homopolymers. WAXD measurements indicated that PPT-PPN copolymers are characterized by isodimorphic cocrystallization. The defect free energies, calculated on the basis of the inclusion model proposed by Wendling and Suter, indicated that the amount of PT units incorporated in the poly(propylene 2,6-naphthalate) (PPN) β crystals is higher than the amount of PN units which cocrystallizes in the poly(propylene terephthalate) (PPT) crystalline phase, probably due to the larger molar volume of PN units compared to PT ones. Amorphous samples showed a monotonic increment of T_g as the content of PN units is increased, due to the stiffening effect of naphthalene rings in the chain. Finally, the Fox equation described well the T_g-composition data.
© 2005 Elsevier Ltd. All rights reserved.

Keywords: Poly(propylene terephthalate/2,6-naphthalate) random copolymers; Thermal properties; Cocrystallization

1. Introduction

Poly(propylene terephthalate) (PPT) has been recently introduced as a commercial polymer, joining the very successful poly(ethylene terephthalate) (PET) and poly (butylene terephthalate) (PBT) on the market. Commercialization was made viable by a breakthrough in the synthesis of the monomer 1,3-propanediol which enabled the polymer to be produced at low costs. Since, 2,6-naphthalene-dicarboxilic acid have been recently produced in large scale, poly(propylene 2,6-naphthalate) (PPN) has also been recognized as an engineering thermoplastics that can be used for fibers, film and molding materials. In this view, PPT and PPN have attracted much interest both from academic and industrial point of view and accordingly

several studies on polymerization kinetics, thermal behavior, crystallization kinetics, crystal structure, rheological and mechanical properties have been reported in the literature [1–10].

The wide diffusion of copolymers for an ever-growing number of industrial applications has given a strong impulse to the study of the correlation between the physical properties and the chemical structure of these materials. Indeed, the knowledge of the structural arrangement of the molecular units is the basis for designing synthetic processes leading to materials with properties tailored to fit specific applications. In particular, the investigation on the thermal properties is fundamental in the improvement of manufacturing processes and consequently of the properties of the polymeric materials obtained. In this view, we synthesized a series of poly (propylene terephthalate/2,6-naphthalate) (PPT-PPN) random copolyesters by reactive blending, starting from PPT and PPN. The present paper reports the results of a detailed molecular, thermal and X-ray diffractometric characterization of these copolymers, carried out in order to study the structure-properties relationships.

2. Experimental

2.1. Reagents

Dimethyl 2,6-naphthalene-dicarboxylatc (NDC) (kindly supplied by AMOCO) and 1,3-propanediol (PD) (Aldrich) were reagent grade products and used as supplied; PPT was kindly purchased in pellet form by Shell Chemicals (USA); titanium tetrabutoxide (Ti(OBu)$_4$, TBT) (Aldrich) was distilled before use.

### 2.2. Synthesis of poly(propylene 2,6-naphthalate)

The synthesis of poly(propylene 2,6-naphthalate) was performed starting from the monomers according to the usual two step procedure for polyester synthesis.

NDC (600.0 g, 2.46 mol) and PD (280 g, 3.68 mol) were introduced in a 250 mL three-neck round-bottom flask, provided with a mechanical stirring, a torque meter and a condenser. TBT (about 0.57 g of Ti(OBu)$_4$/kg of polymer) was added to the reagents and the flask was placed in an oil bath at 150 °C. In the first stage, under pure nitrogen flow, the temperature was increased to 190 °C and kept there until no significant increment in distillate volume was observed (180 min from the catalyst addition). The condenser was removed and the reactor connected to a liquid nitrogen cooled trap. In the second stage, the reaction temperature was increased to 260 °C and a dynamic vacuum was slowly applied. The reaction was conducted at 1 bar until no increase in torque signal was observed (180 min from vacuum application). The molecular weight (M_w) of the synthesized PPN, determined by GPC, turned out to be 50,000. In order to further increase it, a solid-state polymerization was carried out, keeping the polymer, previously pulverized into fine powder, in a vacuum oven for 14 h at 195 °C. In fact a polymer characterized by $M_w = 71,000$ was obtained.

2.3. Synthesis of poly(propylene terephthalate 2,6-naphthalate) copolyesters

Poly(propylene terephthalate 2,6-naphthalate) copolymers of various compositions were obtained by melt mixing, starting from different amounts of PPT and PPN, in presence of 50 ppm of Ti(OBu)$_4$ as catalyst. The two polymers were dried at 100 °C under vacuum and mixed in a 200-mL glass reactor at 260 °C for 60 min under nitrogen atmosphere.

The comonomeric units are the following:
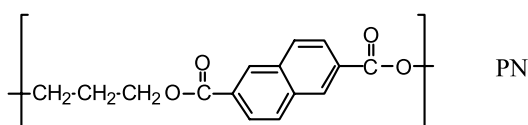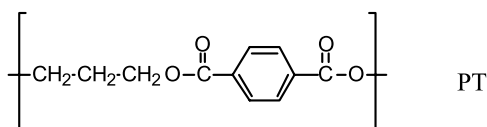
2.4. Infrared and ^{1}H NMR spectroscopy

Infrared spectra were recorded on a 'Spectrum one' FT-IR spectrometer, equipped with an universal ATR sampling accessory on a Di/ZnSe plate.

The chemical structure and composition of PPT-PPN samples were determined by means of ^{1}H NMR spectroscopy, using a Varian INOVA 600 MHz spectrometer. The samples were dissolved in a mixture of trifluoroacetic acid/chloroform-*d* (50/50 v/v) with 0.03% v/v tetramethylsilane added as internal standard.

FT-IR as well as ^{1}H NMR spectroscopy indicate that no side reactions occur during the synthesis of the samples under investigation.

2.5. Gel-permeation chromatography

Molecular weight data were obtained by gel permeation chromatography at 30 °C using a 1100 HP Series system with an UV spectrophotometer (at 254 nm wavelength) as detector, equipped with PL gel 5 μ minimixed-C column. A mixture of dichloromethane/chloroform/1,1,1,3,3,3-hexafluoro-2-propanol (CH$_2$Cl$_2$/CHCl$_3$/HFIP) (75/20/5 v/v/v) was used as diluent with a 0.3 mL/min flow, and sample concentrations of about 10 mg/mL were applied. A molecular weight calibration curve was obtained with several monodisperse polystyrene standards in the range of molecular weight 1000–300,000.

2.6. Wide-angle X-ray measurements

Powder X-ray diffraction measurements were carried out at room temperature with a Bragg/Brentano diffractometer system (Philips PW1050/81-PW1710), equipped with a graphite monochromator in the diffracted beam. Cu anode was used as X-ray source. Data were collected in the range 5–60° (2θ). The crystallinity of each sample was evaluated from the ratio of the integrated crystalline scattering to the total scattering. The background contribution was taken in the due account. The full profile fitting method, in the form of the DEBVIN least-square routine [11,12], was applied to separate the crystalline and amorphous contribution from the total scattering. The crystalline profile was calculated by using the structural data of PPT and β-PPN [2,13]. In each sample two bell-shaped curves, having the form of Pearson VII function, were superimposed to the background segmented line, in order to simulate the amorphous contribution to the total diffracted intensity. The position on the 2θ scale of the bell-shaped curves, their widths and integrated intensities were fitting parameters.

2.7. Thermal analysis

Thermogravimetric analysis was carried out both in air and under nitrogen atmosphere using a Perkin Elmer TGA7

apparatus (gas flow: 50 mL/min) at 10 °C/min heating rate up to 900 °C.

Calorimetric measurements were carried out by means of a Perkin Elmer DSC7 instrument equipped with a liquid subambient accessory and calibrated with high purity standards (indium and cyclohexane). The external block temperature control was set at −60 °C. Weighted samples (ca. 10 mg) were encapsulated in aluminum pans and heated to about 40 °C above fusion temperature at a rate of 20 °C/min (first scan), held there for 3 min, and then rapidly quenched to −10 °C. Finally, they were reheated from −10 °C to a temperature well above the fusion temperature of the sample at a heating rate of 20 °C/min (second scan). The glass-transition temperature T_g was taken as the midpoint of the heat capacity increment Δc_p associated with the glass-to-rubber transition. The melting temperature (T_m) and the crystallization temperature (T_c) were determined as the peak value of the endothermal and exothermal phenomenon in the DSC curve, respectively; when multiple endotherms were observed, the highest peak temperature was taken as T_m. The specific heat increment Δc_p, associated with the glass transition of the amorphous phase, was calculated from the vertical distance between the two extrapolated baselines at the glass transition temperature. The heat of fusion and the heat of crystallization of the crystal phase were calculated from the area of the DSC endotherm and exotherm, respectively. In the case of multiple endotherms, the enthalpy of fusion (ΔH_m) was determined from the total area of DSC endotherms. In order to determine the crystallization rate under non-isothermal conditions, the samples were heated to about 40 °C above fusion temperature at 20 °C/min, kept there for 1 min and then cooled at 5 °C/min. The temperature corresponding to the maximum of the exothermic peak in the DSC cooling-curve (T_{cc}) can be correlated to the crystallization rate. Repeated measurements on each sample showed excellent reproducibility.

3. Results and discussion

At room temperature PPT, PPN and PPT-PPN copolymers appear as semicrystalline solids. Their solubility was checked in various solvents: all the samples were found to be fully soluble at room temperature only in 1,1,1,3,3,3-hexafluoro-2-propanol or in a mixture of dichloromethane/-chloroform/1,1,1,3,3,3-hexafluoro-2-propanol (75/20/5 v/v/v). Before molecular and thermal characterizations, the specimens under investigation were carefully purified by means of the following procedure: after dissolution in dichloromethane/chloroform/1,1,1,3,3,3-hexafluoro-2-propanol (75/20/5 v/v/v) and precipitation in methanol, they were recovered by filtration and again dissolved and reprecipitated twice. Finally, the samples were kept in a vacuum oven at 150 °C overnight in order to remove the residual solvent. The purified polymers are listed in Table 1, which

also collects the weight-average molecular weight (M_w) data, obtained by GPC technique.

The chemical structure of all polyesters was determined by ^{1}H NMR spectroscopy: a typical ^{1}H NMR spectrum is shown in Fig. 1, together with the chemical shift assignments.

In all cases, the spectra were found to be consistent with the expected structure. The copolymer composition was calculated from the relative areas of the ^{1}H NMR resonance peaks of the α-methylene group next to ether–oxygen (a protons) in the range 4.51–4.71 ppm and of the f aromatic protons of the 2,6-naphthalate unit in the range 8.48–8.61 (Fig. 1). The data, summarized in Table 1, show that in all cases the final polymer composition is close to that of the feed.

It is well known that the random or alternate or block nature of copolymers is an important factor which can influence strongly their final properties. Information on the arrangement of the comonomeric units in the chain can be deduced by the degree of randomness b, which can be determined by ^{1}H NMR spectroscopy [14,15]. As can be seen in Fig. 1, the resonance peak of the aromatic protons (f) of naphthalene ring is really constituted by 4 singlets, due to a magnetically different environment, corresponding to NNN, NNT, TNN and TNT sequences resonated at 8.52, 8.54, 8.57 and 8.59 ppm, respectively, where T is terephthalate unit and N is naphthalate one.

The degree of randomness is defined as [15]:

$$b = P_{NNT} + P_{TNN} \tag{1}$$

being:

$$P_{NNT} = I_{NNT}/(I_{NNN} + I_{NNT}) \tag{2}$$

$$P_{TNN} = I_{TNN}/(I_{TNT} + I_{TNN}) \tag{3}$$

where P_{NNT} and P_{TNN} are the probability of finding a T unit next to a N unit and the probability of finding N unit next to a T unit, respectively, and I_{NNT}, I_{NNN}, I_{TNN} and I_{TNT} represent the integrated intensities of the resonance signals of NNT, NNN, TNN and TNT sequences, respectively (and

Table 1
Molecular characterization data of PPT-PPN random copolymers

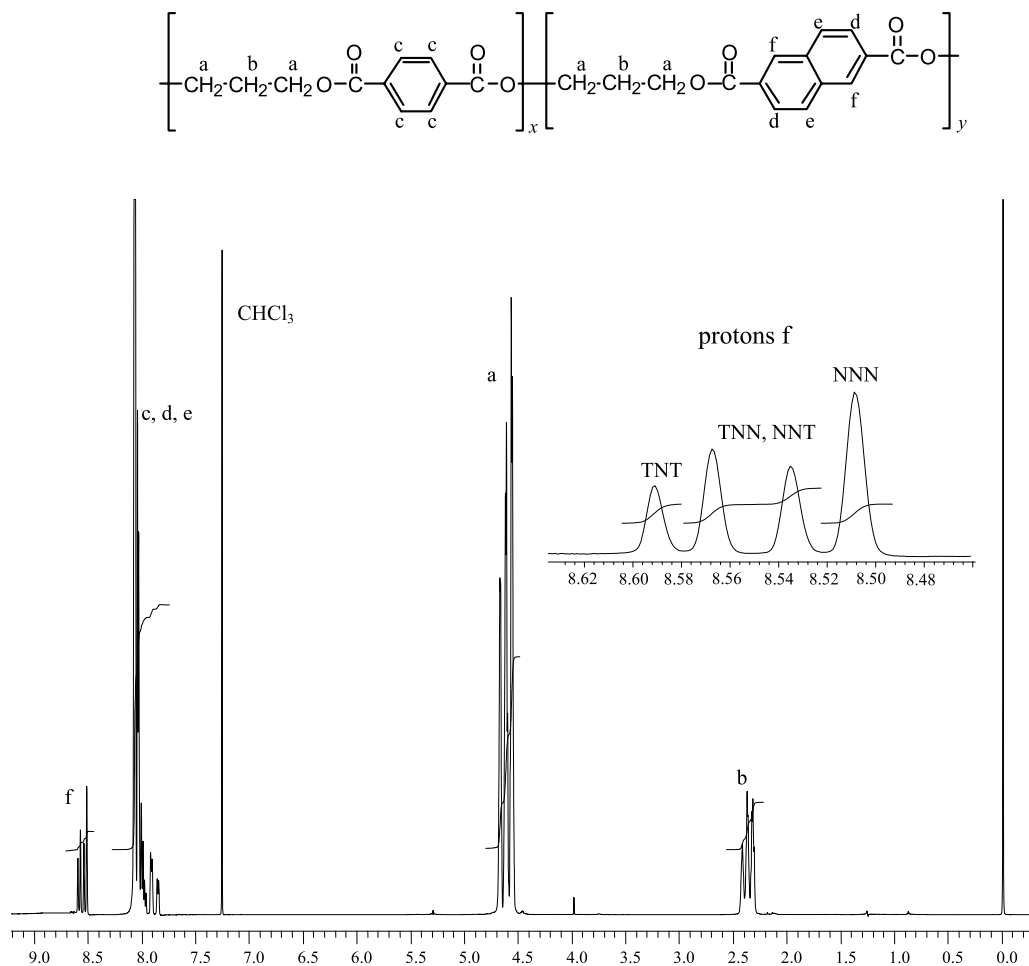| Polymer	PPN (mol%) (feed)	PPN (mol%) (^{1}H NMR)	b	M_w
PPT	0	0.0	–	86,000
PPT-PPN8	8	7.6	0.980	89,900
PPT-PPN15	15	12.9	0.977	82,200
PPT-PPN30	30	30.8	0.972	82,100
PPT-PPN35	35	33.4	0.989	68,600
PPT-PPN45	45	48.6	0.965	70,100
PPT-PPN55	55	50.5	0.977	69,100
PPT-PPN65	65	58.6	0.982	70,200
PPT-PPN75	75	70.0	0.978	70,000
PPT-PPN90	90	85.6	1.089	57,600
PPN	100	100	–	71,000

Fig. 1. 600 MHz ^{1}H NMR spectrum of PPT-PPN45 copolymer and resonance assignments with expansion of interesting aromatic region between 8.48 and 8.62 ppm.

of course $I_{NNT} = I_{TNN}$). It has to be emphasized that b is equal to 1 for random copolymers, equal to 2 for alternate copolymers and is closed to zero for block copolymers.

Table 1 lists the value of b obtained for all samples investigated. In all cases, the degree of randomness was found closed to 1, indicating the random nature of the copolyesters synthesized. The results obtained is not surprising taking into account that with the progress of the interchange reactions occurring during the melt mixing (i.e. for long reaction times) the length of the two different blocks gradually decrease to approach to a statistical distribution of the repeating units [16].

As well known, in almost all polycondensates, cyclic as well as linear molecules are contained in the bulk polymer at the end of the polymerization. In fact, in the ^{1}H NMR spectra of the crude samples under investigation, signals correlated to the presence of cyclic oligomers were detected. It is important to eliminate them for the effects that they might have on some properties, as found in the case of linear and branched poly(ethylene terephthalate) (PET and PETB) [17] and linear and branched poly(butylene isophthalate) (PBI and PBIB) [18]. In particular, in a previous

investigation some of us found for PBI that the purified sample crystallized faster than the as-prepared one. Such difference was just ascribed to the presence of cyclic oligomers in the as-prepared PBI, which behave as defects, hindering the crystalline phase formation. As previously reported for other polyesters [19,20], reprecipitation is a very efficient method to extract cyclic oligomers. As a matter of fact, in the ^{1}H NMR spectra of the purified samples of PPT-PPN copolymers under investigation no trace of the signals due to the protons of the cyclic oligomers was found.

The copolyesters were afterwards examined by thermo-gravimetric analysis and differential scanning calorimetry. The investigation on the thermal stability was carried out both in air and under nitrogen atmosphere. From the thermogravimetric curves in air, the temperature of initial decomposition (T_{id}), the temperature corresponding to the maximum weight loss rate (T_{max}) and the weight loss percent at T_{id} were determined and collected in Table 2.

In all cases, the weight loss takes place practically in one-step and the thermal stability of all the polymers under investigation is quite comparable, being the samples practically stable until to 400 °C. For all PPT-PPN

copolymers the temperature at which the weight loss rate is the highest turned out to be in the range 425–429 °C, with only slight differences with respect to PPT and PPN. Similar behavior was obtained when the TGA measurements were carried out under nitrogen atmosphere.

As regards calorimetric results, being the samples characterized by high and similar M_w, an influence of molecular weight on the glass transition and melting of the polymers synthesized can be excluded.

It is well established that the thermal behavior of a polymer is affected by its previous thermal history and, therefore, each sample was annealed for 24 h at a temperature (T_a) of 30 °C below the corresponding melting temperature (T'_m). As a matter of fact, annealing treatments at the same temperature for different times showed that 24 h are a period of time enough long to develop the highest crystallinity degree in all samples under investigation. The DSC traces of so-treated samples are reported in Fig. 2 and the data obtained in Table 2.

First of all, it can be noted that in all cases multiple melting endotherms are evident. Furthermore, in the copolymers, peak location and heat of fusion appear to depend on composition, both of them assuming the minimum value at the intermediate compositions. In particular, the increase in the amount of comonomer PN or PT added to PPT or PPN, respectively, leads to a decrement of the heat of fusion, indicating a reduced level of crystallinity in the copolymers with respect to the homopolymers. ΔH_m and T_m (relative to the highest temperature melting peak) values are plotted in Fig. 3 as a function of PN unit content, with the exception of PPT-PPN55 whose melting temperature is not reported.

In fact, as shown in Fig. 2, in this case the value is not experimentally detectable, the corresponding high temperature melting peak appearing as a shoulder. Both the minimum in the heat of fusion and the melting point-composition dependence are typical of random copolymers, where both comonomers are able to crystallize, regardless of the fact that the comonomeric units present in minor amount are completely rejected or not from the crystalline phase [21,22]. In most of copolymers, the degree of crystallinity decreases as the minor comonomeric unit content increases, leading often to fully amorphous material even at low comonomer content, due to the incompatibility of the two units in the crystal lattice. On the contrary, if the two crystallizable units are compatible in each crystal lattice, cocrystallization can take place. Cocrystallization behavior in A/B random copolymers is largely classified into two types, i.e. isomorphism and isodimorphism. When the two comonomeric units have similar chemical structures and, therefore, occupy approximately the same volume, the excess free energy for cocrystallization is very small, and, therefore, the chain conformation of both homopolymers becomes compatible with each crystal lattice. Isomorphism develops when only one crystalline phase containing both comonomeric units is detected over all the composition range. On the other hand, copolymers may show isodimorphism, when two crystalline phases are observed. The isodimorphism in its turn is subdivided into two cases. In the former case, each crystalline phase contains both A and B comonomeric units; in the latter case, the A units can cocrystallize with the incorporation of the B comonomeric units, whereas B crystallizes with the complete rejection of the A units. Taking into account that PPT-PPN copolymers show a relevant crystalline phase over the whole composition range, the repeating unit of PPN has similar chemical structure to that of PPT and due to similar crystal structure
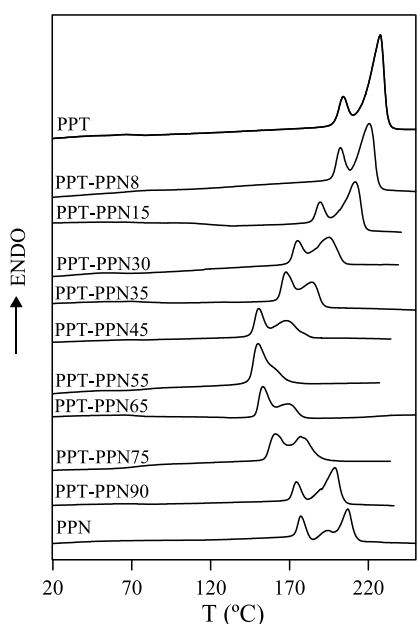

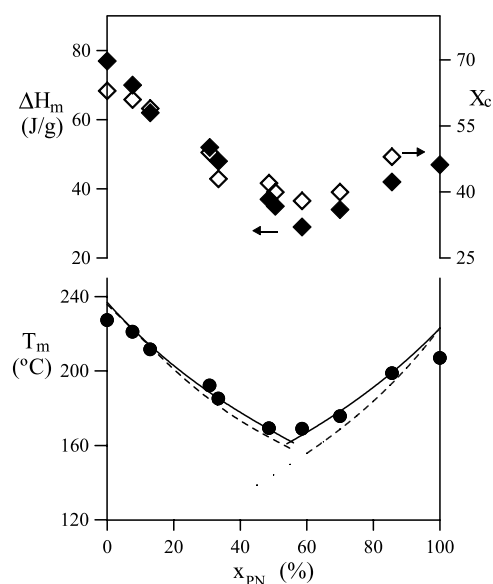Fig. 2. Calorimetric curves of annealed samples.

Fig. 3. Composition dependence of T_m ($\bullet$), ΔH_m ($\blacklozenge$) and X_c ($\diamond$) for PPT-PPN random copolymers. Dashed lines and solid lines represent the Baur model and the Wendling–Suter's model, respectively.

Table 2
Thermogravimetric and calorimetric data of PPT-PPN random copolymers

Polymer	T_{id} (°C)	% at T_{id}	T_{max} (°C)	First scan[a]			Second scan						T_{cc} (°C)
				T_a (°C)	T_m (°C)	ΔH_m (J/g)	T_g (°C)	Δc_p (J/g °C)	T_c (°C)	ΔH_c (J/g)	T_m (°C)	ΔH_m (J/g)	
PPT	410	1.1	429	195	227	77	47	0.396	76	43	225	58	179
PPT-PPN8	409	0.7	427	190	221	70	50	0.354	88	37	214	48	167
PPT-PPN15	406	1.2	425	180	212	62	52	0.349	101	35	211	42	157
PPT-PPN30	408	0.2	427	160	192	52	57	0.334	138	27	190	27	132
PPT-PPN35	411	0.8	427	150	185	48	59	0.325	152	3	183	4	–
PPT-PPN45	407	0.7	425	135	169	37	65	0.310	–	–	–	–	–
PPT-PPN55	410	0.9	427	115	150	35	67	0.304	–	–	–	–	–
PPT-PPN65	408	1.0	428	135	169	29	71	0.292	–	–	–	–	–
PPT-PPN75	407	1.0	426	140	176	34	75	0.283	–	–	–	–	–
PPT-PPN90	406	0.7	428	165	199	42	82	0.272	–	–	–	–	–
PPN	406	0.4	426	175	207	47	87	0.256	–	–	–	–	153

[a] On samples annealed for 24 h at T_a.

and chain conformation of the two polymers, cocrystallization is highly probable. In order to check the nature of the crystalline phase present in the polymers under investigation, X-ray analysis was performed. The data were collected at room temperature and each sample before measurement was annealed for 24 h at T_a. The X-ray diffraction patterns of PPT, PPN and PPT-PPN copolymers are reported in Fig. 4, where both PPT and PPN show well-defined sets of crystalline diffraction peaks.

As previously reported [13], PPN is characterized by two different crystal structures, denoted as α-form and β-form, depending upon the crystallization temperature. By comparing the X-ray profile of the plain PPN with literature data [13], it results that under the applied experimental conditions our sample develops the α-form. As far as the copolymers are concerned, the corresponding WAXD patterns appear to be characterized by relatively intense diffraction peaks over the whole composition range. Moreover, considering the profile shapes, it can be deduced that only one crystalline phase is present in each sample. The patterns can be divided into two groups, according to the PN content: the samples containing from 8 up to 55 mol% of PN
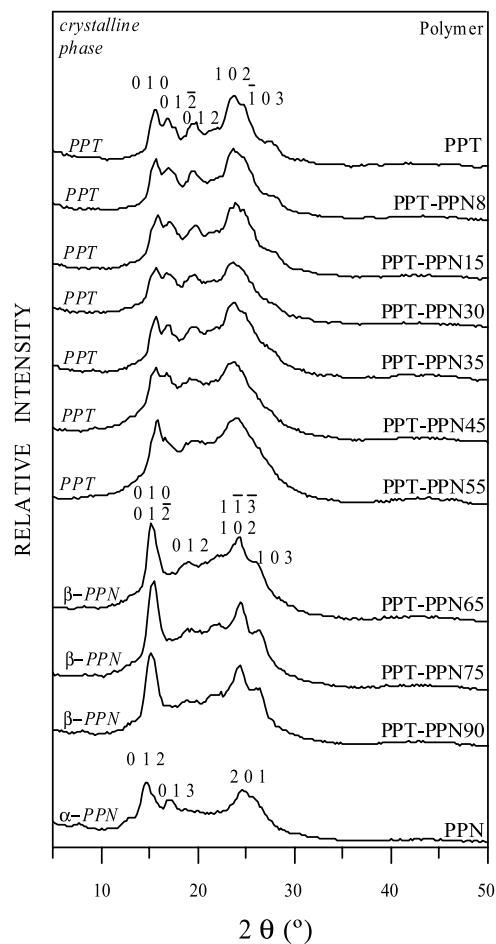

Fig. 4. Wide-angle X-ray diffraction profiles of PPT, PPN and PPT-PPN random copolymers. The indexes of the most intense reflections are reported.

units are characterized by X-ray patterns very similar to that of PPT, indicating that the crystal structure which develops in these copolymers has the characteristics of PPT lattice. On the contrary, the copolymers with PN unit content higher than 55 mol% crystallize assuming the lattice of the PPN β-form. A considerable widening of the diffraction peak width is observed in the copolymers, where the PT/PN ratio approaches to 1, indicating that a shortening of the mean extension of the ordered domains takes place, due to the presence of an increasing number of 'foreign' units which induces defects and less ordered crystals.

It has to be emphasized that the crystal structures of PPT and β-PPN are similar, differing mainly in the *c*-axis dimension and in the β angle value (of the crystalline cell), being indeed the position of the chains relative to the crystallographic axes essentially the same. In this view, and taking also into account that a crystalline phase develops over the whole composition range, cocrystallisation can be hypothesized to occur. In order to check this hypothesis, the crystallinity degree (X_c) was evaluated for all the samples under investigation by means of the fitting procedure described in the Section 2. As an example, a typical plot showing the estimated amorphous contribution to the total intensity profile is shown in Fig. 5 for the PPT-PPN90 sample.

The crystallinity degrees for all the samples are reported in Fig. 3 as a function of composition. It is evident that the copolymerization causes a decrease in the X_c value, indicating that the PN or PT monomeric units are not easily inserted in the crystal lattice of PPT or β-PPN, respectively. However, in all cases, the amount of amorphous fraction turns out to be lower than the value corresponding to the complete rejection of the 'foreign' units from the crystalline phase present in the sample, suggesting, therefore, that at least a certain amount of comonomeric units enter into the crystal lattice.

The transition from PPT type to β-PPN type crystals occurs at a composition near to 55 mol% of PN units, which corresponds to the eutectic composition for the melting temperature. The eutectic composition is defined as the copolymer composition corresponding to the intersection point of the melting temperature curves. Lastly, quite interestingly, the copolymers rich in PN units are characterized by the crystal structure of β-PPN, differently from plain PPN which crystallizes in the α-form. This behavior was already described in the literature in the case of poly(hexamethylene terephthalate-*co*-hexamethylene 2,6-naphthalate) copolymers [23] and for PPT-PPN copolymers could be explained as due to the high likeness between the crystal structures of PPT and β-PPN, permitting, therefore, an easier accommodation of the 'foreign' counits.

Several theories have been developed to explain copolymer crystallization and are commonly classified into two categories: the comonomer exclusion [24,25] and the comonomer inclusion model [26,27]. In particular, when only one counit can crystallize, the second one being completely excluded from the crystals, the melting point reduction is usually examined using Flory's equation. Flory's treatment [24], commonly used in the past and derived assuming that the fusion concerns the disappearance of long sequences of crystallizable units, underestimates the melting point depression of random copolymers. As a matter of fact, the concentration of long sequences decreases with increasing counit content, and the experimental T_m values are consequently lower than postulated by the theory. On the contrary, the equation proposed by Baur [25] takes into account the effect of sequence length of crystallizable units which can crystallize only when their length corresponds to the crystal thickness. Wendling and Suter [28] have recently proposed a new model, which combines the Sanchez–Eby's model [26] (comonomer inclusion model) with the Baur's one [25] (comonomer exclusion model).

The Wendling–Suter equation is given by:

$$\frac{1}{T_m(X_B)} - \frac{1}{T_m^0}$$

$$= \frac{R}{\Delta H_m^0}\left[\frac{\varepsilon X_{CB}}{RT} + (1 - X_{CB})\ln\frac{1 - X_{CB}}{1 - X_B} + X_{CB}\ln\frac{X_{CB}}{X_B} + \langle\tilde{\xi}\rangle^{-1}\right] \quad (4)$$

$$\langle\tilde{\xi}\rangle^{-1} = 2(X_B - X_B e^{-\varepsilon/RT})(1 - X_B + X_B e^{-\varepsilon/RT}) \quad (5)$$

where T_m^0 and ΔH_m^0 are the equilibrium melting temperature and the heat of fusion of homopolymer, respectively, R the gas constant, X_B the molar fraction of B units in the copolymer, X_{CB} that of comonomer B units in the cocrystal, ε the average defect Gibbs free energy, and $\langle\tilde{\xi}\rangle$ the average length of the crystallizable copolymer sequences.

In the equilibrium comonomer inclusion [26,27], the concentration of comonomer B units in the crystal formed
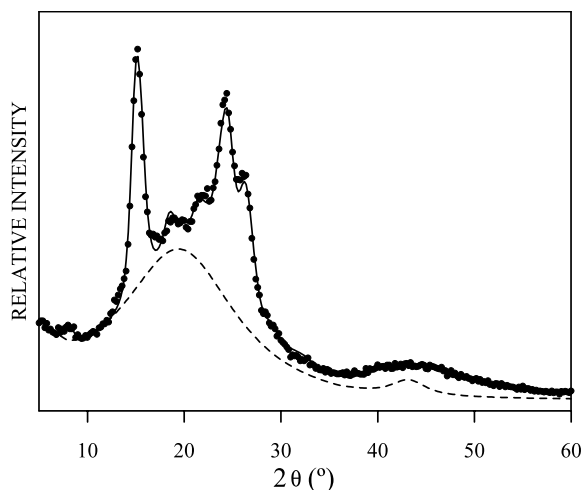
Fig. 5. Graphical output of the least-square routine used in the calculation of the amorphous content of PPT-PPN90. Circles represents the observed intensities, the continuous line the calculated ones. The dashed line is the sum of background and amorphous phase contributions.

by A units is given by:

$$X_{CB}^{eq} = \frac{X_B e^{-\varepsilon/RT}}{1 - X_B + X_B e^{-\varepsilon/RT}} \qquad (6)$$

When X_{CB} in Eq. (2) is substituted by Eq. (4), Eq. (2) turns out to be simplified and becomes:

$$\frac{1}{T_m^0} - \frac{1}{T_m(X_B)}$$
$$= \frac{R}{\Delta H_m^0}[\ln(1 - X_B + X_B e^{-\varepsilon/RT}) - \langle \tilde{\xi} \rangle^{-1}] \qquad (7)$$

when $X_{CB} = X_B$ and $X_{CB} = 0$ ($\varepsilon \to \infty$), Eq. (2) leads to the uniform inclusion model and the exclusion model (the Baur's model), respectively.

As shown in Fig. 3, the Wendling–Suter equation (Eq. (7)) fits well the experimentally determined melting points of the copolymers, using for PPT $T_m^0 = 237\ ^\circ C$ and $\Delta H_m^0 = 30$ kJ/mol [29] and for PPN β crystal $T_m^0 = 223\ ^\circ C$ and $\Delta H_m^0 = 26$ kJ/mol [13]. In the same figure, the theoretical curve obtained on the basis of Baur's model is also drawn for sake of comparison: the experimental data of PPT-PPN copolymers are in general higher than the predicted values, the discrepancy being more relevant at high content of the counits present in the copolymer. Moreover, it can be noted that the difference between the experimental and theoretical melting points is higher for the copolymers that crystallize in the PPN β type crystal lattice.

From the intersection of the melting temperature curves, the eutectic composition is estimated to be in correspondence of 55 mol% PN, in perfect agreement with the results obtained by means of the X-ray diffraction measurements and reported above. The Wendling–Suter's equilibrium inclusion model can be also employed to determine the average defect free energy. This latter was found to be 0.318 and 0.907 kJ/mol for the homopolymers PPT and PPN, respectively. As can be seen, the value of ε corresponding to the incorporation of PT units into PPN crystal lattice is higher, indicating that the amount of PT units incorporated in PPN β-form crystals is much higher than the amount of PN units which cocrystallizes in the PPT crystalline phase. This is probably due to the larger molar volume of the PN units compared to the PT ones. As a result, the PN units accommodate themselves into PPT crystal lattice with a certain difficulty. On the contrary, the PT units are readily incorporated into PPN β type crystal lattice.

By using Eq. (3) with the defect free energies and the T_m's of the copolymers, the concentration (X_{CB}) of comonomeric units in the cocrystal can be estimated. When X_{CB} is plotted against X_B, as shown in Fig. 6, one can observe that the comonomer concentration in each crystal lattice increases with increasing the comonomer composition in the bulk.

In both cases, however, the comonomer concentration in each crystal lattice is lower than that based on the uniform inclusion model ($X_{CB} = X_B$), indicating that a fraction of the
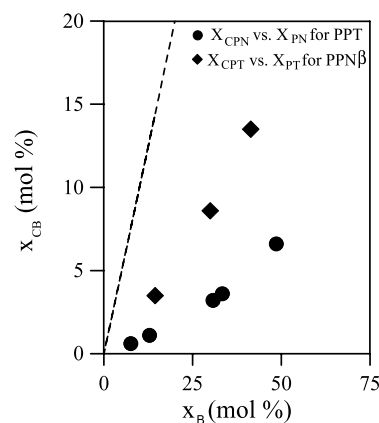

Fig. 6. Concentration of PN and PT units incorporated in the PPT and PPN crystals, respectively, as a function of copolymer composition. The dashed line is based on the uniform inclusion model.

comonomeric units is rejected in the amorphous phase. These results appear in agreement with those obtained by means of X-ray diffraction measurements.

As mentioned above, multiple melting peaks are present in the DSC traces of PPT, PPN and PPT-PPN copolymers (Fig. 2). It is worth remembering that the multiple melting peaks has been the subject of intense studies and has given rise to much controversy. At present, two main hypothesis have been proposed to take into account for this phenomenon: (i) melting and recrystallization processes occurring during the calorimetric scan [30–32] and (ii) existence of different crystal structures [33–35]. As well known from the literature [3,36,37], the multiple melting endotherm phenomenon observed in PPT and PPN has been ascribed to a reorganization process taking place during the DSC scan, due to a mechanism based on melting and recrystallization of less perfect crystallites into thicker crystals, followed by a final melting process at higher temperature. Therefore, the multiple melting peaks present in the DSC traces of the copolymers can be hypothesized to have the same origin. In order to confirm the possibility of melting–recrystallization processes, the effect of the heating rate on the melting phenomenon was evaluated. As shown in Fig. 7, the magnitude of melting peak I increases as the heating rate is increased, contrarily to the high temperature melting peak II, the intensity of which regularly decreases with increasing the heating rate.

The higher value of the heat of fusion of the melting peak I at the faster heating rate indicates that the crystals formed at T_c have not enough time to melt and recrystallize, confirming, therefore, the mechanism based on melting and recrystallization of less perfect crystallites into thicker crystals melting at higher temperature [31]. Moreover, analyzing in more detail the Fig. 2, one can observe that the ratio between the area of the lowest temperature melting peak to the highest temperature one appears to depend on composition, increasing as the amount of PN or PT counits added to PPT or PPN, respectively, is increased. In the case
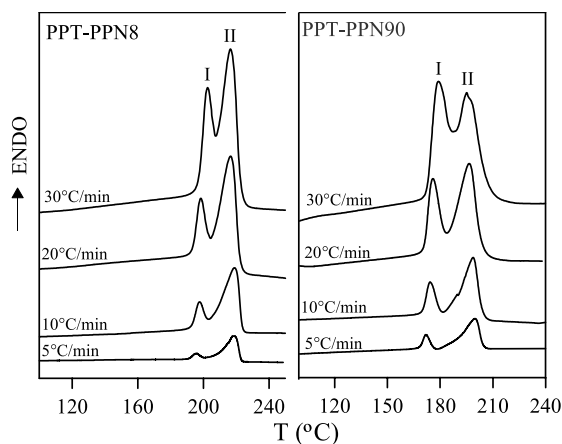
Fig. 7. DSC melting endotherms of PPT-PPN8 and PPT-PPN90 (annealed for 24 h at T_a) scanned at the indicated heating rates. The curves have not been corrected for changes in the instrumental signal with heating rate.
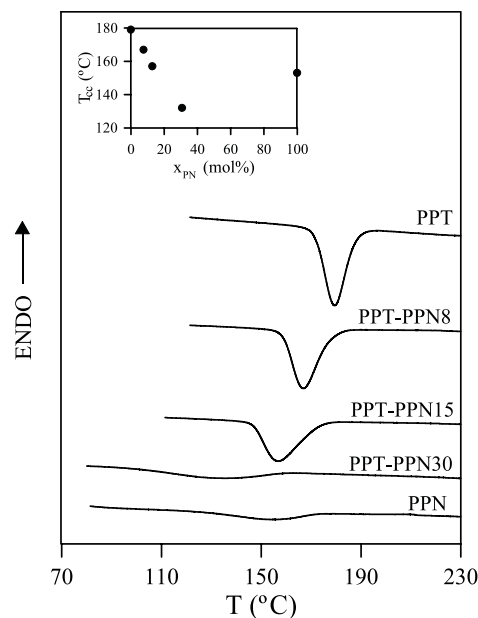

Fig. 8. DSC crystallization exotherms of PPT and PPN and PPT-PPN random copolymers cooled from the melt at 5 °C/min. In the inset: T_{cc} as a function of PN unit content.

of PPT-PPN55 copolymer, only one endotherm with a shoulder is evident. The observed trend suggests that the occurring of the recrystallization process is influenced by the comonomer unit content, being the phenomenon practically hindered by the presence of a relatively high content of 'foreign' units (as in the case of PPT-PPN55). In order to obtain a confirmation of this hypothesis the crystallization kinetics under non-isothermal conditions was analysed (for the details see Section 2). It is worth remembering that the half-time of primary crystallization in isothermal experiments correlates with the temperature of the maximum of the crystallization peaks in non-isothermal experiments (T_{cc}) [38], being this latter more easily obtainable. The exothermic crystallization peaks of the samples under investigation are shown in Fig. 8, with the exception of the copolymers containing from 90 to 35 mol% of PN units being these samples not able to crystallize even though cooled from the melt at low rate (5 °C/min).

Such behavior indicates, therefore, that in these copolymers the crystallization rate of PPN or PPT is significantly decreased by the presence of comonomeric units. In particular, a low amount of PT units (10 mol%) is sufficient to depress completely the crystallisation process of PPN under the adopted experimental conditions. Moreover, it can be observed, as also shown in the inset, reporting T_{cc} values as a function of composition, that the temperature of the maximum of the exothermal crystallization peak regularly decreases as the PN unit content is increased. This fact indicates a decrement of the overall crystallization rate of PPT, due to the presence of counits which act as obstacles in the regular packing of polymer chains.

It is well known that a partially crystalline material usually exhibits a different glass transition behavior than the completely amorphous analogous. In fact, although some conflicting results are reported in the literature [39], crystallinity usually acts like cross-linking and raises T_g through its restrictive effect on the segmental motion of

amorphous polymer chains. Therefore, in order to study the influence of chemical structure on the glass transition of random copolymers, the phenomenon should be examined in the total absence of crystallinity. In this view, all the samples under investigation were subjected to rapid cooling (quenching) from the melt (see Section 2 for the details). In order to completely prevent crystallization and obtain polymers in a completely amorphous condition, each sample was quenched outside the calorimeter cell by immersion in liquid nitrogen as quickly as possible. As a matter of fact, such method permits a faster cooling with respect to that obtained inside the DSC equipment. The DSC curves after melt quenching are shown in Fig. 9: the calorimetric traces of PPT and PPT-PPN copolymers containing up to 35 mol% of PN units show a glass transition followed by an exothermal 'cold crystallization' peak and a melting endotherm at higher temperature.

As concern PPT, PPT-PPN8 and PPT-PPN15, the enthalpy associated with the crystallization phenomenon is lower than that of the fusion endotherm, indicating that these samples cannot be frozen into a completely amorphous state by quenching. The DSC curves of such samples are, therefore, typical of partially crystalline polymers. As a matter of fact, it is well known that PPT cannot be easy frozen in an amorphous glassy state due to its high rate of crystallisation [40].

In the case of PPT-PPN30 and PPT-PPN35, the enthalpy of crystallization very well compares with the corresponding heat of fusion, indicating that both copolymers are completely amorphous. As regards the calorimetric curves of pure PPN and copolymers containing from 45 to 90 mol% of PN units, only an intense endothermal baseline

deviation associated with the glass transition is observed. Therefore, the DSC scans indicate a quite different thermal behavior of PPN and PPT homopolymers: in fact, the former is completely amorphous, whereas the latter is partially crystalline. Moreover, the phase behavior of PPT-PPN copolymers depends on composition: as a matter of fact, after melt quenching, semicrystalline samples are exclusively obtained at high PPT content. As can be seen in Fig. 9 and from the data collected in Table 2, the glass transition temperature is influenced by the amount of PN units in the chain. The values of T_g are plotted in Fig. 10 as a function of PN unit content. The values of T_g of partially crystalline PPT and PPT-PPN copolymers containing 8 and 15 mol% of PN units do not follow the same composition dependence as that of the amorphous samples: in fact, the measured glass transition temperature value is higher than expected, the crystallites hindering the motion of the amorphous chains. As far as the trend of the glass transition temperature with the composition is concerned, one can observe that T_g values increase as PN unit content is increased, due to the stiffening effect of naphthalene rings in the polymeric chain.

In amorphous random copolymers, T_g is usually a monotonic function of composition [41] and the most common relationship used to predict T_g as a function of comonomer content is the Fox equation [42]:

$$1/T_g = w_I/T_{gI} + w_{II}/T_{gII} \qquad (8)$$

where T_{gI} and T_{gII} are the glass transition temperatures of the pure homopolymers and w_I and w_{II} the respective weight fractions.
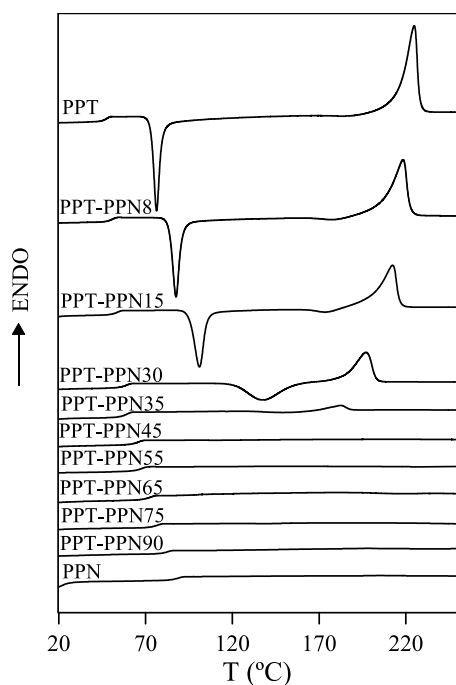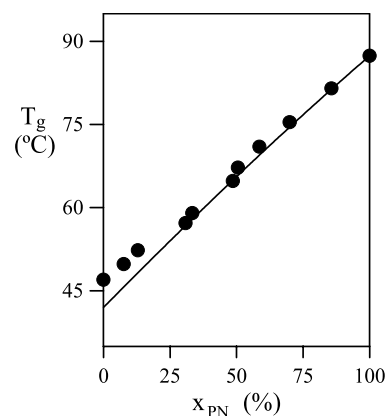
As shown in Fig. 10, the equation fits well the

Fig. 10. Composition dependence of T_g for PPT-PPN random copolymers; theoretical curves of T_g vs. composition calculated on the basis of Fox equation (solid line).

experimental data of the completely amorphous samples, using for PPN the glass transition temperature experimentally measured by us, and fixing for PPT the value of 42 °C, reported in the literature [29].

4. Conclusions

A series of PPT-PPN random copolymers with different composition were obtained by melt mixing, an easy and rapid method of preparation. The investigations carried out on this copolymeric system lead to some interesting results on the effect of comonomeric units on the thermal properties of PPT and PPN. Composition appears to be the prominent parameter in determining the characteristics of the samples under investigation. The thermal stability, crucial factor during the processing of a polymeric material, was found to keep good for all the copolymers. Both calorimetric and WAXD results indicate that PPT-PPN copolyesters showed an isodimorphic cocrystallization behavior, the samples crystallizing in either of the PPT or PPN lattices, depending on composition, and the crystalline phase being conspicuous over the whole composition range. All experimental evidences agree in locating the eutectic composition in the vicinity of 55 mol% of PN units content. The T_m values appear to be well correlated to composition by Wendling–Suter's equation, permitting the determination of the average defect free energies for the homopolymers PPT and PPN; the value of ε corresponding to the incorporation of PT units into PPN crystal lattice was found to be higher, indicating that PPN crystal lattice accommodates higher amounts of propylene terephthalate units. Moreover, the applicability of Wendling–Suter's equation can be considered a further, even though indirect, evidence of the occurring of cocrystallization in the copolymers under investigation. The compatibility of the two crystallizable comonomeric units with each crystal lattice (i.e. cocrystallization) can be considered an interesting

Fig. 9. Calorimetric curves of PPT, PPN homopolymers and their random copolymers after melt quenching.

result, since, it is expected that thermal and mechanical properties of the copolymer can be controlled without significant loss of crystallinity through the variation of the copolymer composition. As far as the melting phenomenon is concerned, multiple endotherms were found in the copolymers, similarly to PPT and PPN; such behaviour was ascribed to a reorganization process occurring during the DSC scan. Interestingly, the kinetics of recrystallization process appeared to be affected by composition, its rate becoming lower as the amount of 'foreign' units was increased. As a matter of fact, non-isothermal crystallisation kinetics studies showed that the rate at which crystallinity develops strongly depends on composition too, being slower when the copolymer composition is close to the eutectic one. The DSC scans performed after rapid cooling from the molten state, indicate a quite different thermal behavior of PPN and PPT homopolymers, the former being completely amorphous, the latter partially crystalline. As far as the copolymers are concerned, their behavior appears to be strongly affected by composition, amorphous or semicrystalline samples being obtained at high PPN or high PPT content, respectively. Lastly, amorphous samples showed a monotonic increase of the glass transition temperature as the amount of PN units is increased, due to the stiffening effect of naphthalene rings in the polymeric chain.

In summary, the present results clearly support the occurrence of cocrystallization in PPT-PPN copolymers and point out concomitant impressive composition effects on the thermal properties.

References

[1] Traub HL, Hirt P, Herlinger H, Oppermann W. Angew Makromol Chem 1995;230:179.
[2] Desborough IJ, Hall IH, Neisser JZ. Polymer 1979;20:545.
[3] Sisti L, Finelli L, Lotti N, Berti C, Munari A. e-Polymers 2003;054.
[4] Jakeways R, Ward IM, Wilding MA. J Polym Sci Polym Phys Ed 1975;13:799.
[5] Schultz JM, Wu J. 2002 In: Fakirov S, editor. Handbook of thermoplastic polyesters, vol. 1. Germany: Wiley-VCH, chapter 12.
[6] Tsai RS, Lee YD. J Polym Res 1998;5(2):77.
[7] Hwang SK, Yeh C, Chen LS, Way TF, Tsay LM, Liu KK, et al. Polym Prepr 1999;40:611.
[8] Stier U, Gahr F, Oppermann W. J Appl Polym Sci 2001;80:2039.
[9] Stier U, Oppermann W. J Polym Sci: Part B Polym Phys 2001;39:620.
[10] Stier U, Schawaller D, Oppermann W. Polymer 2001;42:8753.
[11] Immirzi A. Acta Cryst 1980;B36:2378.
[12] Brückner S, Immirzi A. J Appl Cryst 1997;30:207.
[13] Jeong YG, Jo WH, Lee SC. Polymer 2004;45:379.
[14] Devaux J, Godard P, Mercier JP. J Polym Sci Polym Phys Ed 1982;20:1875.
[15] Chen MS, Chang SJ, Chang RS, Kuo WF, Tsai HB. J Appl Polym Sci 1990;40:1053.
[16] Marechal E. 2002 In: Fakirov S, editor. Handbook of thermoplastic polyesters, vol. 2. Germany: Wiley-VCH, chapter 1.
[17] FarrowsE G, Hill ES, Weinle PL. Encyclopedia of polymer science. vol. 11. New York: Wiley; 1969.
[18] Finelli L, Lotti N, Munari A. J Appl Polym Sci 2002;84(11):2001.
[19] Wick G, Zeitler H. Angew Makromolek Chem 1983;112:59.
[20] Pilati F, Munari A, Manaresi P, Dilani G, Bonora V. Eur Polym J 1987;23:265.
[21] Mandelkern L. Crystallization of polymers. New York: McGraw-Hill; 1954.
[22] Mandelkern L. In: Allen G, Bevington JC, editors. Comprehensive polymer science, vol. 2. Oxford: Pergamon Press; 1989 [chapter 11].
[23] Lee JH, Jeong YG, Lee SC, Min BG, Jo WH. Polymer 2002;43:5263.
[24] Flory PJ. Trans Faraday Soc 1955;51:848.
[25] Baur H. Makromol Chem 1966;98:297.
[26] Sanchez IC, Eby RK. Macromolecules 1975;8:638.
[27] Helfand E, Lauritzen JI. Macromolecules 1973;6:631.
[28] Wendling J, Suter UW. Macromolecules 1998;31:2516.
[29] ATHAS Data Bank. Pure Appl Chem 1995;67:1919 http://web.utk.edu/~athas/.
[30] Blundell J, Osborn BN. Polymer 1983;24:953.
[31] Lee Y, Porter RS. Macromolecules 1989;22:1756.
[32] Rim PB, Runt JP. Macromolecules 1984;17:1520.
[33] Marand H, Alizadeh A, Farmer R, Desai R, Velikov V. Macromolecules 2000;33:3392.
[34] Chung JS, Cebe P. Polymer 1992;33:2312.
[35] Lemstra PJ, Schouten AJ, Challa G. J Polym Sci Polym Phys Ed 1974;12:1565.
[36] Huang JM, Chang FC. J Polym Sci: Part B Polym Phys 2000;38:934.
[37] Wu PL, Woo EM. J Polym Sci: Part B Polym Phys 2002;40:1571.
[38] Legras R, Bailly C, Daumerie M, Dekoninck JM, Mercier JP, Zichy V, et al. Polymer 1986;27:109.
[39] Boyer RF. Rub Chem Tech 1963;36:1303.
[40] Berti C, Bonora V, Colonna M, Lotti N, Sisti L. Eur Polym J 2003;39:1595.
[41] Eisenberg A. Physical properties of polymers. Washington, DC: ACS; 1984.
[42] Fox G. Bull Am Phys Soc 1956;1:123.